JOURNAL OF NATURAL REMEDIES
DOI: 10.18311/jnr/2024/36288

RESEARCH ARTICLE

Development and Characterisation of Curcuminoid Loaded Hydrogel for the Effective Treatment of Diabetic Retinopathy

Durga Prasad Kondeti[1] and T. Sundarrajan[2*]

[1]SRM College of Pharmacy, SRM Institute of Science and Technology, Kattankulathur – 603203, Tamil Nadu, India

[2]Department of Pharmaceutical Chemistry, SRM College of Pharmacy, SRM Institute of Science and Technology, Kattankulathur – 603203, Tamil Nadu, India; chemistrysundar@gmail.com

Abstract

Background: The leading cause of vision loss in individuals with diabetes worldwide is diabetic retinopathy. A curcuminoid-loaded hydro gel has been proposed to improve solubility and ocular permeation. **Aim:** A gel-based formulation using gellan gum was hypothesised to enhance its bioavailability. The RP-HPLC analysis confirmed curcuminoid isolated from raw turmeric. **Methods:** By varying the gellan gum concentrations, three different formulations were developed. The developed curcuminoid-loaded gel formulation was further characterised by its FT-IR signature analysis, particle size, zeta potential, morphology and *in-vitro* release behaviour. **Results:** The signature analysis results indicate a drug's signature in the formulation. The study revealed sphere-sized particles ranging from 6387±113 to 4595±184 nm with zeta potential ranging from -21 ±2.29 mV to -19.6 ±3.19 mV. A sustained release pattern was observed by the *in-vitro* release studies. The results of *ex vivo* corneal permeation studies indicate that the developed curcuminoid loaded hydrogel have some exposure to the posterior segment of the eye. **Conclusion:** To conclude the developed curcuminoid hydrogel may provide exposure to the posterior segment of the eye due to its significant corneal permeation property.

Keywords: Curcuminoid, Diabetic Retinopathy, Dispersion, Hydrogel Formulation

1. Introduction

Diabetic patients face an eye condition called diabetic retinopathy[1]. For both type 1 and type 2 diabetes mellitus this seems to be a highly specific vascular complication. High blood glucose causes alteration of the blood-retina with a thickened basement membrane. Damage to the retina is associated with Diabetic retinopathy. Sometimes abnormal new blood vessels grow on the retina, considerably reducing vision. Proliferative Diabetic Retinopathy (PDR) and Non-Proliferative Diabetic Retinopathy (NPDR) are the two types of DR (Diabetic Retinopathy)[2-4]. PDR can reduce both the central and peripheral (side) vision. NPDR is an early stage of diabetic eye disease. If you have NPDR you have a blurry vision.

One of the primary components of the rhizome of *Curcuma longa* (L) and other *Curcuma* species is curcuminoid. Curcuminoid comprises 77% of two additional related compounds, dimethoxy curcuminoid and bis-dimethoxy curcuminoids in the form of diarylheptanoids which exist as bright orange-yellow crystalline compounds[5-10]. These are used as a food additive and colouring agents. As prescribed by WHO, the daily intake as a food additive ranges from 0–3mg/kg. They are being used as anticancer agents which are soluble in polar and nonpolar organic solvents, alkali and extremely acidic solvents like glacial acetic acid, but are nearly insoluble in water at acidic and neutral pH values[11-14]. The compound is 1,7-bis(4-hydroxy-3-methoxyphenyl)-1,6-heptadiene-3,5-dione (Figure 1). The melting point is 183 °C, and the molecular weight

*Author for correspondence

Article Received on: 17.01.2024 Revised on: 04.05.2024 Accepted on: 28.06.2024

is 368.38. Dalton was associated with curcuminoid. Turmeric has long been used to treat a variety of illnesses, especially against inflammation. Curcuminoid is effective against inflammation, cancer treatment, microbial infections, hepatic protection, nephron protection, thrombosis, myocardial infarction, rheumatoid arthritis, glucose lowering and acts against oxidation 1,22. At higher doses, curcuminoid was found to be safe[15-18].

The microbe *Sphingomonas elodea* formerly known as *Pseudomonas elodea*, secretes gellan gum, an extracellular polysaccharide. It is produced commercially through a fermentation process[19-20]. Gellan gum is of two types, Low Acyl (LA) and High Acyl (HA). When hot solutions are cooled with gel-promoting cations present, gellan gum forms gels at low concentrations. Gellan gum is a water-soluble anionic polysaccharide produced by *Pseudomonas elodea*, which is composed of a repeating unit of monomers, tetrasaccharide, that are two residues of D-glucose and one of each residue of D-glucuronic acid and L-rhamnose[21-24]. Gellan gum products are generally classified into two categories, LA and HA depending on the number of acetate groups attached to the polymer[25-27].

The present work aims to develop the poorly water-soluble curcuminoid into a curcuminoid-loaded hydrogel which seems to be soluble in water and is expected to enhance ocular bioavailability.

2. Materials and Methods

Curcuminoid, Gellan gum, Potassium hydrogen phosphate, Sodium hydroxide and Ethanol, were obtained From Sigma Aldrich. All buffers and solutions were prepared with distilled water.

2.1 Extraction of Curcuminoid

The turmeric collected from the North Eastern region of India was shade-dried and pulverised. and the coarse powder was treated along with petroleum ether for dewaxing and removal of chlorophyll. This was subject to a continuous hot percolation process for 8 hours, and it was packed (250g) in a soxhlet apparatus using 450mL of ethanol (95% v/v) as solvent. Under reduced pressure and controlled temperature (50°C) in a rotary evaporator, the extract was concentrated to dryness.

A 50-gram dry ethanol extract was suspended in a 1:4 ethanol-to-water mixture. Petroleum ether, chloroform and ethyl acetate were the solvents used in a sequential liquid-liquid partitioning process to extract the resultant solution in an increasing order of polarity. After gathering all the fractions, the solvents were extracted using a rotary evaporator set at a temperature of ± 40° C. The resulting extracts were then stored in vacuum desiccators until needed again.

2.2 HPLC Analysis of Curcuminoid

RP-HPLC was used to estimate the isolated curcuminoid (Shimadzu prominence made up of LC 20 AD). On an analytical column made of Phenomenex Luna C18 (250×4.6 mm, 5µ), chromatographic separation was accomplished. Curcuminoid was diluted accurately using ethanol followed by dilution in pH 7.4 buffer. The mobile phase of methanol: 0.1% trifluoro acetic acid (50:50% v/v) was used at a flow rate of 1ml/min. The UV detection was carried out at 420nm. The retention time of curcuminoid was found to be 5.4.

3.3 *In vitro* Antioxidant Assay

3.3.1 DPPH Radical Scavenging Activity

An equal volume of the ethanolic extract containing curcuminoid in methanol at varying concentrations was added to 1mL of a 100.0 µM DPPH solution in methanol and it was left in the dark for 30 minutes. A spectrophotometer was used to measure the colour shift in terms of absorbance at 514nm. The control tube was filled with 1mL of methanol instead of the test sample. Ascorbic acid in varying concentrations served as the reference substance. Using the equation, the percentage of inhibition was determined.

$$\frac{\text{Absorbance of control - Absorbance of test}}{\text{Absorbance ofcontrol}} \times 100$$

3.4 FT-IR Analysis

The compatibility of curcuminoid, gellean gum and hydrogel was recorded using an FTIR spectrometer (PERKIN ELME). FTIR samples were prepared by the KBr pellet method using a hydraulic pellet press and scanned over a range of 4000cm^{-1} to 400cm^{-1}.

3.5 Development of Curcuminoid Loaded Hydrogel

Gellan gum was dissolved in 10ml methanol at different concentrations (50, 25, 10mg). Then stirred for 1 hour at 700rpm. A weighed amount of curcuminoid (2mg)

dissolved in methanol was injected dropwise into the gellan gum solution and stirred at 700 rpm for 24 hours. The formed curcuminoid-loaded hydrogel was stored at 4°C for further analysis.

3.6 Encapsulation Efficiency of Curcuminoid Hydrogel

Encapsulation of curcuminoid in curcuminoid-loaded hydrogel was estimated using UV - a visible Spectrophotometer. Curcuminoid hydrogel of 0.2µl was treated with methanol and sonicated for 15 minutes further diluted with pH 7.4 buffer and using a UV spectrophotometer and the absorbance was measured at 420nm.

3.7 Particle Size and Zeta Potential Analysis

Particle size and charge of curcuminoid loaded hydrogel were performed by Malvern Zeta Seizer (Malvern NANO zs series).100µl of resultant formulation were dissolved in milli Q water (2ml)[28].

3.8 Transmission Electron Microscope (TEM) Analysis

A TEM equipped with JEM-20100 (JEOL, JAPAN) was used to examine the precise morphology of the developed hydrogel. A drop of the diluted DEX-NDs was applied to a copper grid that had been coated with carbon to create the TEM sample, which was then observed.

3.9 Stability Studies for Curcuminoid Hydrogel

Over 30 days, the *in vitro* stability of curcuminoid hydrogel was tested at various temperatures, including room temperature (37°C) and refrigeration (5°C). Following their respective conditions, the sample's particle size and zeta potential were measured.

3.10 *In Vitro* Release Studies

The curcuminoid hydrogel was checked for its release by using the dialysis bag method (using a 12,000–14,000 molecular weight cut-off limit dialysis membrane). 200µl of curcuminoid-loaded hydrogel was treated with 800 µl of pH 7.4 buffer. The setup was kept under a magnetic stirrer at 200 rpm and release samples (ml) were collected at different time intervals (5 minutes to 8hours) during each time point. 1.0ml of phosphate buffer pH 7.4 was replaced accordingly. The collected samples were analysed using a UV-visible spectrophotometer at 428nm.

3.11 *Ex Vivo* Corneal Permeation Study

The side-by-side diffusion cell with a donor and receptor compartment was used to study corneal permeation. After obtaining the goat eyes from the slaughterhouse, Phosphate Buffer Saline (PBS) was used to rinse them. Using a 1-millilitre tuberculin syringe, the vitreous humour of the removed eye was extracted and forceps were used to separate the cornea. During the experiments, the adhered scleral portion that remained after the cornea was carefully removed was used to hold the tissue in place between the half cells.

After being cleaned with PBS, the removed cornea was positioned vertically on the donor half-cell, endothelium facing the reservoir solution. The donor half-cell was clamped after being positioned vertically over the receptor half-cell. A circulating water bath was used to keep the temperature constant at 34°C during the investigations. PBS (pH 7.4) was added to the reservoir chamber and the prepared hydrogel was placed in the donor chamber. Magnetic stir bars were used to constantly stir the contents of both chambers. The recipient chamber's volume was intentionally kept higher than the donor chamber's to allow the hydrostatic pressure differential to preserve the cornea's inherent curvature. Three-milliliter aliquots of the sample were taken out of the receiver chamber at predetermined intervals. The collected samples were analysed by using a UV Spectrophotometer at 425nm.

4. Results and Discussions

4.1 Preliminary Phytochemical Screening

The preliminary phytochemical screening revealed that the ethanol extract contains carbohydrates, phytosterols, alkaloids, glycosides, saponins, flavonoids, phenolic compounds and terpenoids. Among the fractions, ethyl acetate fraction contains many phytochemical constituents and the yield was also found to be high when compared to other fractions as shown in Table 1.

4.2 HPLC Analysis of Curcuminoid

Isolated curcuminoid was estimated using RP-HPLC (Shimadzu prominence consisting of LC 20 AD) as shown in Figure 1.

Table 1. Preliminary phytochemical screening of various extracts

Phytochemical Constituents	Name of the Extract				
	Ethanol Extract	Petroleum Ether	Chloroform	Ethyl Acetate	Water
Carbohydrates	+	-	-	+	+
Phytosterols	+	+	-	-	-
Alkaloids	+	-	+	+	-
Glycosides	+	-	-	+	+
Terpenoids	+	+	+	-	-
Proteins and Aminoacids	+	-	+	+	+
Saponins	-	-	-	-	-
Tannins	+	-	-	+	+
Flavonoids	+	-	-	+	+

(+) Presence (-) Absence

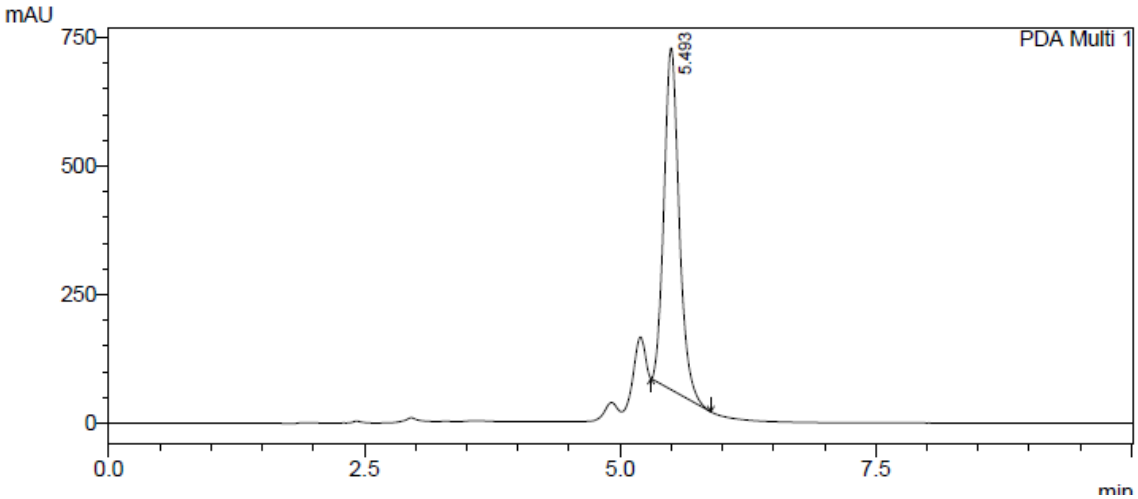

Figure 1. HPLC chromatogram of curcuminoid.

4.3 *In vitro* Antioxidant Study

The effect of curcuminoid on DPPH was estimated. The results indicate that the curcuminoid has very potent DPPH radical scavenging activity (75.52%) when compared with control, ascorbic acid.

4.4 Compatibility Analysis

The drug compatibility investigation was done with FT-IR. FT-IR analysis requires checking the signature of curcuminoid presence in the developed formulation. In this case, the structural and functional groups of the generated CURNGs were examined using FT-IR analysis. The OH of carbohydrates is represented by the characteristic absorption band 34.3559cm^{-1} that CURNGs displayed, proteins and polypeptides groups Further CURNGs showed bands at 1639.44cm^{-1} due to C=O amide bond and 711.19 cm^{-1} due to para-distributed benzes bonds. Gellan gum showed absorption bands 3444.82 cm^{-1} corresponding to the OH of carbohydrates, proteins polypeptides groups. Further Gellan gum showed bands at 2922.34 cm^{-1} due to C-H methyl ring bonds. CU showed absorption bands 34.36.55cm^{-1} OH of carbohydrates, protein and polypeptides groups. CU showed bonds at 2922.98 cm^{-1} C-H methyl ring 2922.98 cm^{-1}, 2853.26 cm^{-1} (Table 2) due to CH and CH_2 aliphatic stretching groups were presented. The results of FT-IR analysis show the compatibility nature of CU, CURNGs and gellan gum designated for the formulations (Figure 2).

Table 2. FT-IR compatibility analysis and its functional groups

Absorption Frequency (cm^{-1})	Stretching Group	Functional Group
34.3559 cm^{-1}	O-H Stretch	Carboxylic Acids
1639.44 cm^{-1}	C=O	Carbonyl Group
711.19 cm^{-1}	C-Br	Alkyl Amines
2922.34 cm^{-1}	C-H Stretch	Aromatic Amines
34.3655 cm^{-1}	O-H Stretch	Carboxylic Acids
2922.98 cm^{-1}	C-H Stretch	Aromatic Amines
2853.26 cm^{-1}	C-H Stretch	Aromatic Amines

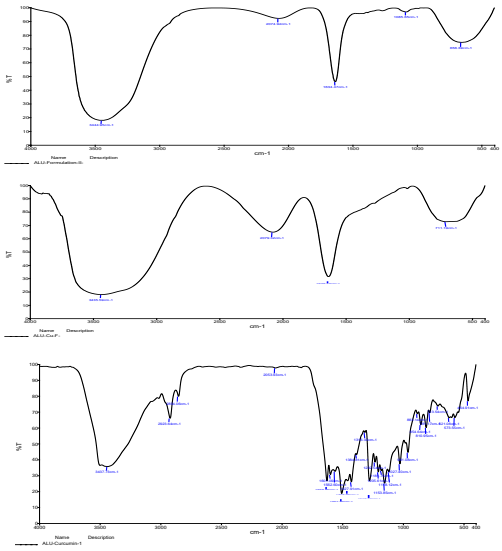

Figure 2. FT-IR compatibility analysis of (A) curcuminoid, (B) gellan gum, and (C) curcuminoid-loaded hydrogel formulation.

4.5 Formulation Development of Curcuminoid Loaded Hydrogel Formulation

Using gellan gum, the curcuminoid-loaded hydrogel was created. Gellan gum offers even more functional properties and applications when combined with other gums or polymers, which can be done with ease. Gellan concentration typically increases with gel strength. Gellan gum keeps its strength at 90°C and is stable at high temperatures. Eliminating organic solvents from the formulation could have a significant effect. Three distinct formulations (10mg, 25mg and 50mg) were created by varying the concentration of gellan gum. These formulations were then examined for size, zeta potential and encapsulation efficiency (Table 3). Size, zeta potential and encapsulation efficiency were taken into consideration when selecting the optimal formulation.

4.6 Particle Size and Zeta Potential Analysis

For each of the three CUR-NGs (CUR-NGs-1 to CUR-NGs 3), the particle size and zeta potential varied from 6387±113 to 4595±184 (Table 3). According to Figure 3, the zeta potential is between -21 ±2.29 mV and -19.6 ±3.19 mV. As the concentration of gellan gum (50mg, 25mg, or 10mg) increases, the size of CUR-NGs particles also increases. Furthermore, compared to lower concentrations (10mg), a higher concentration of gellan gum (50mg) is needed to produce CURNGs with smaller particle sizes. In certain cases, the reduction in interfacial stability caused by insufficient gellan gum in the CURNGs formulation could be the cause of the increase in particle size, potentially resulting in hydrogel aggregation. The influence of a negatively charged formulation may not have a positive impact on the mucin present on the surface of the eye.

4.7 Encapsulation Efficiency of CURNGs

The peak was observed at the retention time of Rt 5.4 which indicates the presence of curcuminoid. In general, higher drug encapsulation is desired to achieve a better therapeutic effect on the target site. The amount of curcumin present in CUR-NGs was determined for three different formulations (CURNGs-1 to CURNGs3). The lower zeta potential (-19.6 ± 3.19) with a higher amount of CURNGs encapsulation from encapsulation (21.3±2.29) for CUR-NGs-2 has been selected for further studies.

4.8 TEM Analysis

The morphology of CURNGs as analysed by TEM showed a spherical morphology as indicated in Figure 4.

4.9 *In Vitro* Release of CURNGs

The UV visible spectrophotometer was used to analyse the CUR-NGs' *in vitro* release. Measurements of cur release and an assessment of the viability of employing CUNGs to the target site were made after CURNGs were exposed to pH (corresponding to physiological pH)

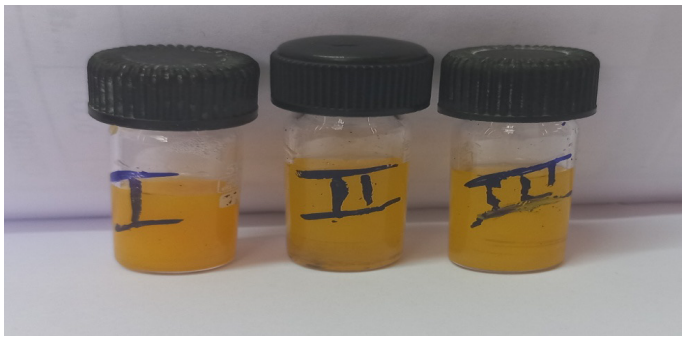

A

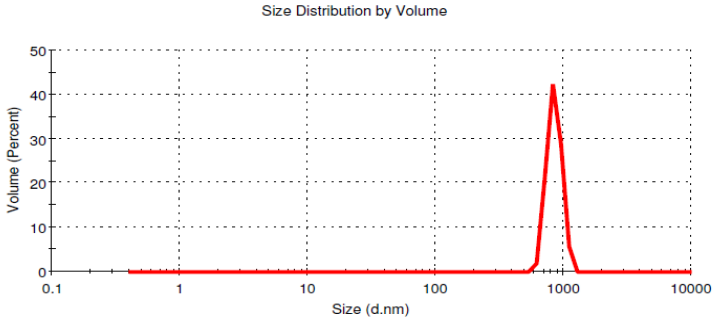

B

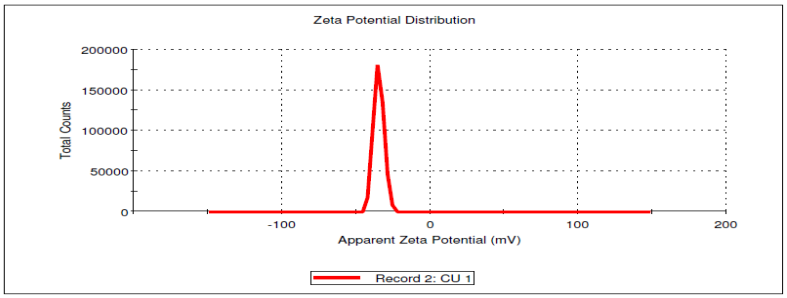

C

Figure 3. Size distribution graph and zeta potential of CUR-NGs.

Table 3. *In vitro* characterization results of CURNGs

Formulation Code	Gellan Gum (mg)	Average Particle Size (nm) ± SD	Zeta Potential (mV) ± SD	CURNGs Amount in (mg) ± SD
CURNGs-1	50mg	6387±1130	-21.3±2.29	0.70±0.01
CURNGs-2	25mg	4595±1843	-20.4±2.57	3.00±0.10
CURNGs-3	10mg	6387±1130	-19.6±3.19	3.11±3.25

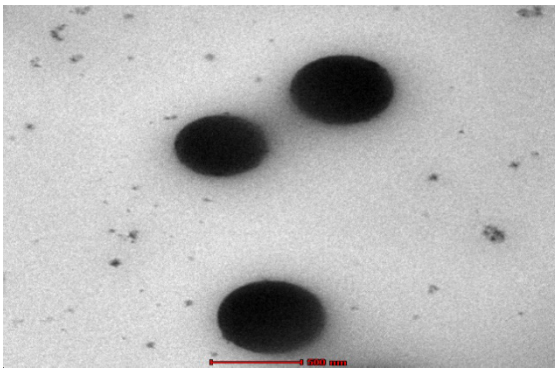

Figure 4. Morphology of CURNGs.

conditions at 37°C. The release of the drug is contingent upon several experimental factors, including but not limited to pH, degradation rate, particle size, drug-surface interaction and polymer behaviour. The CURNGs showed an initial release of 0.128 ±0.006 within 5 minutes, followed by 82.11±11.76351 within 30 minutes, followed by 199.70±92.65439 5h, 0.376±0.104 after 8 hours. This kind of initial higher drug release may be useful in maintaining higher CU concentration and may aid in drug transport across the skin. This formulation offers a sustained release pattern as shown in Figure 5.

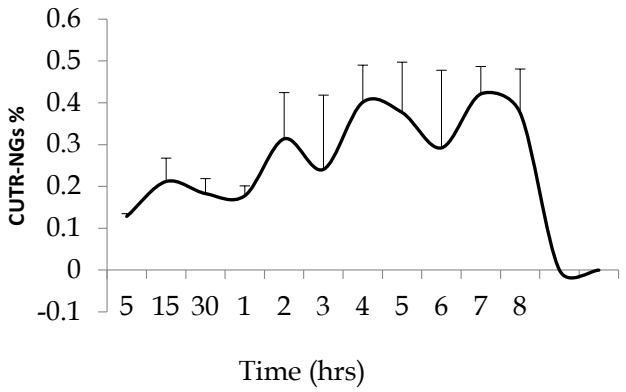

Figure 5. *In vitro* release studies of CUR-NGs.

4.10 Stability Analysis

In vitro studies showed that there was an increase in particle size observed for 24 hours and 30 days respective to the initial particle size values.

4.11 *Ex Vivo* Corneal Permeation Study

The mean drug permeation across the cornea following a single dose of CUR- NGs-2 represents that 0.00131 mg curcumin has been permeated within 120 minutes, which indicates that the developed formulation containing curcumin has shown permeation at the posterior pole of the eye.

5. Discussion

Several nanoformulations on curcumin have been reported in this study. Fe_3O_4 nanoparticles, measuring 6nm in size, were coated with Folic Acid (FA) and Hyperbranched Polyglycerol (HPG) has been reported. In contrast to non-functionalised nanoparticles, the functionalised nanoparticles (10–20 nm) exhibited a lower propensity to aggregate. The drug-loading processes using curcumin were compared between HPG@Fe_3O_4 and FA@HPG@Fe_3O_4 nanoparticles. The maximum drug-loading capacities of HPG@Fe_3O_4 and FA@HPG@Fe_3O_4 nanoparticles were found to be 88% and 82%, respectively[25]. Zinc oxide-grafted curcumin nanocomposites (ZNP–Cs) have been recently reported for their anti-microbial action. Assays for antimicrobials were performed on both gram-positive and gram-negative bacterial stains. The investigation's findings show that the synthesised nano matrix can function as a potent, additively improved combination of delivery and therapeutic agent with potential applications in cancer treatment and other biological fields[26]. Mesoporous Silica Nanoparticles (MSNs) loaded with curcumin have demonstrated potential as drug delivery vehicles to overcome the restricted pharmacokinetic properties of curcumin. Pegylation and functionalisation with FA improve permeability, stability, biocompatibility and anticancer activity. Co-administration of other medications leads to a synergistically increased cytotoxic effect[27]. It has been reported that loading Rat Tracheal Epithelial (RTE) cells with curcumin-loaded methoxy polyethylene-glycols-poly (lactic-co-glycolic acid) nanoparticles (Cur-mPEG-PLGA-NPs) reverses corticosteroid resistance brought on by Cigarette Smoke Extract (CSE). Hydrophilic polymer networks-based hydrogels exhibit the capacity to absorb and retain aqueous fluids and hold significant promise in biomedical applications owing to their high water content, permeability and structural similarity to the extracellular matrix[28]. Recent reports suggest that redox-degradable hydrogel loaded with an antibacterial peptide (vancomycin) using disulfide bond-containing hyperbranched polyglycerol (SS-hPG) is cross-linked by 4-arm polyethene glycol-thiol (4-arm PEG-SH)[29].

6. Conclusion

This study talks about curcumin-loaded hydrogel (CUR-NGS) for the treatment of Diabetic retinopathy. In this work, we describe the hydrogel of curcumin expected to enhance its ocular bioavailability. Since curcumin is a natural hydrophobic polyphenol, it has low aqueous solubility and bioavailability, which are challenging to its therapeutic efficiency. The developed formulation at future may be checked for its efficacy using retinal epithelial cell lines with a scope of utility in the near future.

7. Acknowledgement

The authors gratefully acknowledge the support received from SRM College of Pharmacy, SRMIST, Chennai, Tamil Nadu.

8. References

1. Witmer AN, Vrensen GF, Van Noorden CJ, Schlingemann RO. Vascular endothelial growth factors and angiogenesis

in eye disease. Prog Retin Eye Res. 2003; 22:1-29. https://doi.org/10.1016/S1350-9462(02)00043-5 PMid:12597922.
2. Evans JR, Michelessi M, Virgili G. Laser photocoagulation for proliferative diabetic retinopathy. Cochrane Database Syst Rev. 2014; 11:CD011234. https://doi.org/10.1002/14651858.CD011234
3. Osaadon P, Fagan XJ, Lifshitz T, Levy J. A review of anti-VEGF agents for proliferative diabetic retinopathy. Eye (Lond). 2014; 28(5):510-20. https://doi.org/10.1038/eye.2014.13 PMid:24525867 PMCid: PMC4017101.
4. Gonzalez-Cortes JH, Martinez-Pacheco VA, Gonzalez-Cantu JE, Bilgic A, de Ribot FM, Sudhalkar A, Mohamed-Hamsho J, Kodjikian L, Mathis T. Current treatments and innovations in diabetic retinopathy and diabetic macular oedema. Pharmaceutics. 2022; 15(1):122. https://doi.org/10.3390/pharmaceutics15010122 PMid:36678750 PMCid: PMC9866607.
5. Venkatesan N. Curcumin attenuation of acute adriamycin myocardial toxicity in rats. British J Pharmacol. 1998; 124(3):425-7. https://doi.org/10.1038/sj.bjp.0701877 PMid:9647462 PMCid: PMC1565424.
6. Aggarwal S, Takada Y, Singh S, Myers JN, Aggarwal BB. Inhibition of growth and survival of human head and neck squamous cell carcinoma cells by curcumin via modulation of nuclear factor-κb signalling. Int J Cancer. 2004; 111(5):679-92. https://doi.org/10.1002/ijc.20333 PMid:15252836.
7. Anand AB, P, Sundaram C, Jhurani S, Kunnumakkara Aggarwal BB. Curcumin and cancer: an "old-age" disease with an "age-old" solution. Cancer Letters. 2008; 267(1):133-64. https://doi.org/10.1016/j.canlet.2008.03.025 PMid:18462866.
8. Anand P, Kunnumakkara AB, Newman RA, Aggarwal BB. Bioavailability of curcumin: problems and promises. Mol Pharm. 2007; 4(6):807-18. https://doi.org/10.1021/mp700113r PMid:17999464.
9. Basnet P, Skalko-Basnet N. Curcumin: an anti-inflammatory molecule from a curry spice on the path to cancer treatment. Molecules. 2011; 16(6):4567-98. https://doi.org/10.3390/molecules16064567 PMid:21642934 PMCid: PMC6264403.
10. Chen A, Xu J, Johnson AC. Curcumin inhibits human colon cancer cell growth by suppressing gene expression of epidermal growth factor receptors through reducing the activity of the transcription factor egr-1. Oncogene. 2006; 25(2):278-87. https://doi.org/10.1038/sj.onc.1209019 PMid:16170359.
11. Chen J, Tang XQ, Zhi J, Cui Y, Yu HM, Tang EH, Sun SN, Feng JQ, Chen, PX.Curcumin protects pc12 cells against 1-methyl-4-phenylpyridinium ion-induced apoptosis by bcl-2-mitochondria-ros-inos pathway. Apoptosis. 2006; 943-53. https://doi.org/10.1007/s10495-006-6715-5 PMid:16547587.
12. Gupta SC, Prasad S, Kim JH, Patchva S, Webb LJ, Priyadarsini LK, Aggarwal BB. Multitargeting by curcumin as revealed by molecular interaction studies. Nat Product Rep. 2011; 28(12):1937-55. https://doi.org/10.1039/c1np00051a PMid:21979811 PMCid: PMC3604998.
13. Hanahan D, Weinberg RA. Hallmarks of cancer: the next generation. Cell. 2011; 144(5): 646-74. https://doi.org/10.1016/j.cell.2011.02.013 PMid:21376230.
14. Joint FA. Evaluation of certain food additives and contaminants: sixty-first report of the joint fao/who expert' committee on food additives. World Health Organization. 2004.
15. Kiso Y, Suzuki Y, Watanabe N, Oshima Y, Hikino H. Antihepatotoxic principles of *Curcuma longa* rhizomes. Plantamedica. 1983; 49(11):185-7. https://doi.org/10.1055/s-2007-969845 PMid:6657788.
16. KwakHS, Yang KM, Ahn J. Microencapsulated iron for milk fortification. Jagri Food Chem. 2003; 51(26):7770-4. https://doi.org/10.1021/jf030199 PMid:14664543.
17. Lemmon MA, Schlessinger J. Cell signalling by receptor tyrosine kinases. Cell. 2010; 141(7):1117-34. https://doi.org/10.1016/j.cell.2010.06.011 PMid:20602996. PMCid: PMC2914105.
18. Parimita SP, Ramshankar YV, Suresh S, Guru Row TN. Redetermination of curcumin: (1e, 4z, 6e)-5-hydroxy-1, 7-bis (4-hydroxy-3-methoxyphenyl) hepta-1, 4, 6-trien-3-one. Actacrystallographica section e. Structure Reports Online. 2007; 63(2):o860-2. https://doi.org/10.1107/S160053680700222X
19. Jansson PE, Lindberg B, Sandford PA. Structural studies of gellan gum, an extracellular polysaccharide elaborated by *Pseudomonas elodea*. Carbohydr Res. 1983; 124:135-9. https://doi.org/10.1016/0008-6215(83)88361-X
20. Osmalek T, Froelich A, Tasarek S. Application of gellan gum in pharmacy and medicine. Int J Pharm. 2014; 466:328-40. https://doi.org/10.1016/j.ijpharm.2014.03.038 PMid:24657577.
21. Bacelar AH, Silva-Correia J, Oliveira JM, Reis RL. Recent progress in gellan gum hydrogels provided by functionalisation strategies. J Mater Chem B. 2016; 4(37):6164-74. https://doi.org/10.1039/C6TB01488G PMid:32263628.
22. Chakraborty S, Jana S, Gandhi, A, Sen, KK, Zhiang W, Kokare C. Gellan gum microspheres containing a novel alpha-amylase from marine *Nocardiopsis* sp. strain B2 for immobilisation. Int J Biol Macromol. 2014; 70:292-9. https://doi.org/10.1016/j.ijbiomac.2014.06.046 PMid:25014636.
23. Mahdi MH, Conway BR, Smith AM. Development of muco adhesive sprayable gellan gum fluid gels. Int J Pharm. 2015; 488(1-2):12-19. https://doi.org/10.1016/j.ijpharm.2015.04.011 PMid:25863119.
24. Rosas-Flores W, Ramos-Ramirez EG, Salazar-Montoya JA. Microencapsulation of *Lactobacillus helveticus* and

Lactobacillus delbrueckii using alginate and gellan gum. Carbohydr Polym. 2013; 98(1):1011-17. https://doi.org/10.1016/j.carbpol.2013.06.077 PMid:23987441.

25. Farani MR, Azarian M, Sheikh Hossein HH, Abdolvahabi ZAH, Mohammadi Abgarmi, Moradi ZA, Mousavi SM, Ashrafizadeh M, Makvandi P, Mohammad Saeb R, Rabiee N. Folic acid-adorned curcumin-loaded iron oxide nanoparticles for cervical cancer. ACS Appl Bio Mater. 2022; 5(3):1305-18. https://doi.org/10.1021/acsabm.1c01311 PMid:35201760 PMCid: PMC8941513.
26. Perera WPTD, Dissanayake RK, Ranatunga UL, Hettiarachchi NM, Perera KDC, Unagolla JM, De Silva RT, Pahalagedara LR. Curcumin-loaded zinc oxide nanoparticles for activity-enhanced antibacterial and anticancer applications. RSC Adv. 2020; 10(51):30785-95. https://doi.org/10.1039/D0RA05755J PMid:35516060 PMCid: PMC9056367.
27. Iranshahy M, Hanafi-Bojd MY, Aghili SH, Iranshahi M, Nabavi SM, Saberi S, Filosa R, Nezhadi IF, Hasanpour M. Curcumin-loaded *Mesoporous silica* nanoparticles for drug delivery: synthesis, biological assays and therapeutic potential - a review. RSC Adv. 2023; 13(32):22250-67. https://doi.org/10.1039/D3RA02772D PMid:37492509 PMCid: PMC10363773.
28. Chen X, Wang D, Guo X, Li X, Ye W, Qi Y, Gu W. Curcumin-loaded mPEG-PLGA nanoparticles attenuates the apoptosis and corticosteroid resistance induced by cigarette smoke extract. Front Pharmacol. 2022; 25(13):824652. https://doi.org/10.3389/fphar.2022.824652
29. Mariam C, Paraskevi SS, Zainab A, Tatyana LP, Boonya T, Xin F, Ehsan M, Rainer H. Redox-responsive hydrogels loaded with an antibacterial peptide as controlled drug delivery for healing infectious wounds. J Appl Polym Sci. 2021; 24:1-10.